Modelling Lane Keeping by a Hybrid Open-Closed-Loop Pulse Control Scheme

***Abstract*—This paper presents a novel methodology for modelling human lane keeping control by characterizing a unique concept of *elementary steering pulses*, which are motor primitives in man-vehicle systems. The novelty of the paper is the introduction of *elementary steering pulses* that have been evidently extracted from *naturalistic driving data* through machine learning techniques (data-driven modelling), and are incorporated into an alternative steering control scheme. This newly proposed hybrid-open-closed- loop (HOCL) control scheme, where an *elementary steering pulse* starts with an open loop, representing real human's reflex responses triggered by human lane keeping errors, and is adjusted back with the traditional close-loop control, has shown a significant improvement on both the stability and matching performance to real driving events. Online measurement of the key metrics in the steering process provides a new tool for monitoring driver states, and the biofidelic steering model may provide human-like qualities for future automated lane-keeping systems. Both will add to the array of tools available for achieving autonomous and semi-autonomous driving systems, which greatly benefits the current vehicle industry.**

***Index Terms*—Driver behaviour, man-machine systems, open-closed- loop control systems, road safety, biofidelic modelling, data-driven modelling.**

I. Introduction

THE way in which humans manoeuvre a vehicle is a complicated task which involves initially the interpretation of all the sensory information about the road conditions ahead. It is generally accepted that visual stimuli account for 90% of the sensory information used by the driver to choose the required driving action [1]. In fact, the central nervous system (CNS) can easily control the manoeuvres of a vehicle using only this information. Human driving modelling in the literature [2] is generally based in linear control laws acting in closed-loop as a response to a visually perceived lane keeping error. This category of steering control models, although can exhibit good driving from a performance point of view can hardly characterize normal human driving, which is essentially a nonlinear task. In this paper, through signal processing and machine learning techniques we extract *elementary steering pulses* from *naturalistic driving data* (NDD) and incorporate them in a new framework of steering control through *data-driven modelling* – patterns in data are identified to construct a biofidelic representation of human steering control. The purpose is to suggest new assistance and automation control technologies, by understanding how humans perform steering corrections to keep the vehicle within the lane boundaries or to avoid potential road conflicts.

A. Related Work

From the point of view of modelling driver behaviour, one fundamental question is: which are the road distinctive attributes or which are the regions of the road ahead from which the driver extracts the most significant information. Early experiments performed more than fifty years ago on test-tracks [3], showed that the visual information from a particular sighting distance is of special importance for human lane keeping in straight roads. The required sighting distance depends on the speed of the vehicle, height of the driver and also on local driving habits. Furthermore, experiments in curved test-tracks suggested that the driver focuses sight at a different distance according to road curvature [3]. Later literature [4] [5], advocated that drivers typically use information from 'near' and 'far' regions of the road relative to the vehicle, to produce a suitable steering wheel action. This led to Salvucci and Gray to propose a linear steering control model [6], which is discussed in this paper and compared with the newly formulated approach. In distinction to the two point strategy of Salvucci and Gray for modelling driving behaviour, other models have been suggested in the literature. Many of these are surveyed in [1] and [2]. Beyond these models, one alternative approach to conventional control methods is the 'act-and-wait' method [7] [8], which is incorporated into the proposed control scheme.

Steering signals obtained from NDD [9] do indicate that steering actions consist of a series of relatively short pulse-like corrections rather than smooth, linear and continuous steering motion [10]. It has been verified [11] that hand movement in reaching behaviour follows a bell-shaped pattern over time. As a consequence, it has been hypothesized that motor movements are composed by adding different motor primitives [12]. In [13] it is shown that steering corrections can be fitted by Gaussian functions and that they can be described by superposition of symmetric motor primitives. Thus, a new model is required which explicitly includes such motor primitives. In [14], such a model of steering control was introduced, and here it is developed further by deriving the required steering action primitives directly from NDD.

Signal processing of steering signals has been applied to vehicle industry extensively; some examples are the *steering entropy* [15], a driver workload measure developed by Nissan Motor Co. Ltd, and the *Driver Alert Control* developed by Volvo, a monitoring system of driver vigilance. It should also be mentioned that in addition to vehicle control and *conditional automation* another approach, the *electronic stability control* (ESC), increases vehicle stability through braking control to help in the steering [16].

There is an immense interest in developing vehicles that take over the steering control from the driver in particular situations, for example in highway cruising; this comes under the heading of *conditional automation* – or level 3 of automation in the scale from 0 to 5 according to the specification of the

Society of Automotive Engineers (SAE) [16]. Although fully automated vehicles (level 5) seem unlikely for unconditional use in a very near future, *conditional automation* is a more feasible and immediate goal. This level of automation involves a transition of control between driver and vehicle that, in order to be safe, must happen in a smooth manner. There must be a period of transition in which the vehicle holds some of the steering control, and the driver must be sympathetic to it while holding the steering wheel. For this to be possible, a better understanding of how humans drive is needed.

B. Contribution

In this paper, existing tools in signal processing and control theory are integrated to extract the natural pulses occurring in NDD. An exhaustive analysis, as the one presented, applying signal processing and machine learning techniques to steering patterns has not occurred before in the literature. The extracted pulses are incorporated into an already existing pulse control law [14] to propose a new nonlinear hybrid open-closed loop (HOCL) control scheme. Therefore our approach has been one of *data-driven modelling*. The HOCL control scheme performs an initial steering pulse correction in open-loop which is later ended in a closed-loop control action, in an analogous way as how the CNS appears to work. Unlike previous driver control models, the driving strategy of this scheme is extracted from NDD and not conceptualized merely from theoretical considerations.

The key contributions of the presented work are: (i) to introduce new means of driver steering control that characterize normal human driving and are thus biofidelic, (ii) to propose a new framework for driver assistance and level 2 (partial automation) or 3 (conditional automation) of vehicle control [16], and (iii) to expose the industrial applications of the new methods.

In the following (Section II) the characteristics of the NDD used are explained along with the description of the simulations. Section III evaluates the Salvucci and Gray model where its parameters are fitted with NDD. In Section IV the natural patterns in the steering pulses – *elementary steering pulses* – are extracted from NDD, and the length of the rising and falling parts of such pulses is determined. This leads us to propose the HOCL control scheme based on *elementary steering pulses*, alternative to the conventional linear control laws. In Section V, the generic HOCL scheme is formulated and an example is developed to compare stability and performance with respect to the Salvucci and Gray model – with parameters fitted from NDD. Finally, conclusions are drawn, and future work is suggested in Section VI.

II. Experimental Data and Simulations

It is only recently that rich databases of naturalistic driving data have become available for research [9],[17]. Here, the source of the data is the Road Departure Crash Warning (RDCW) Field Operational Test [17]. For the present analysis and parameter estimation, 200 sets of data were used, corresponding to 200 driving events for 4 different drivers (50 for each). The data are considered 'naturalistic', that is, the data are recorded in real road conditions where subjects don't have to interact with the logging equipment, and eventually become unaware of it. Thus the data represent 'normal' driving. The recorded data comprises around 400 channels including dynamic data variables – recorded at $10\,\mathrm{Hz}$ – and video based recordings such as lane tracking at $2\,\mathrm{Hz}$. Each of the events has a duration of 60 seconds. The four drivers (A, B, C, D) are all within the age range from 40 to 50 years old. Drivers (A, B) are female while drivers (C, D) are male. The initial speed of the events is $28 - 32\,\mathrm{ms}^{-1}$ with an overall variation less than $\pm 5\,\mathrm{ms}^{-1}$. The driving events were recorded in roads essentially straight, with radius of curvature at least $500\,\mathrm{m}$.

For parameter fitting the data have been utilized at the sampling frequency – $10\,\mathrm{Hz}$ – but for machine learning analysis the data have been interpolated to $30\,\mathrm{Hz}$. Comparison simulations with fitted parameters run accordingly at $10\,\mathrm{Hz}$ and are performed in closed-loop between the steering control model and a linear bicycle vehicle model. The NDD events were recorded in Nissan Altima 3.5SE (2003) vehicles, thus the parameters of the vehicle model were adjusted according to the specifications of this model of vehicle. A yaw moment perturbation on vehicle response was added, so that the steering control model could not simply point the vehicle straight and cease action. The amplitude of the perturbation was adjusted to be equivalent in magnitude to the one found in the NDD.

To create a realistic control problem and allow the simulation to test a biofidelic driving pattern, a delay of $200\,\mathrm{ms}$ is introduced; this was included in the simulations performed to fit model parameters between the driver control and the vehicle. The delay represents the effect of neuromuscular processes in the human driver. At the same time, the driver control responds to future predicted stimuli according to the road conditions by using the yaw rate and vehicle velocity. The prediction is also set at $200\,\mathrm{ms}$ in the future to counteract the response lag. This therefore represents a lag compensation for visual cues, but not to motion cues such as yaw rate response to perturbations in the vehicle. The chosen response time is comparable to the reported value of $180\,\mathrm{ms}$ in reference [1]. These considerations are important because it is well known that delays in the CNS [18], and in control systems in general [19], decrease the stability of the system.

III. Two Point control model

The Salvucci and Gray model, simplifies the notions of 'near' and 'far' regions of the road in the form of a near and a far point fixed at given distances. According to the model, the driver makes two type of corrections, one to keep the vehicle within the lane edges, according to the angle from the heading of the vehicle to a near point θ_n, and the other to accommodate the trajectory of the vehicle to the road geometry according to the angle to a far point θ_f. The near point is always at the centre of the lane, while the far point can also be the tangent point from the vehicle position to the farthest visible point of the curve when the road is not straight [6]. In the present analysis we consider only roads which are essentially straight (see Section II), so here it is considered that the far point is

again at the centre of the lane. The Salvucci and Gray control law is the following:

$$\dot{\delta} = K_f\dot{\theta}_f + K_n\dot{\theta}_n + K_i\theta_n \tag{1}$$

where δ is the steering angle.

This approach, while explaining many aspects of human lane-keeping, has some limitations. The control law (1) responds to the errors in a continuous manner. As soon as an error is detected the controller tries to rectify it. Additionally, the controller reacts simultaneously to information from the 'near' and the 'far' regions of the road. Another important remark is that the controller is linear.

For parameter fitting the discrete version of equation (1) is considered [6]:

$$\Delta\delta = K_f\Delta\theta_f + K_n\Delta\theta_n + K_i\theta_n\Delta T \tag{2}$$

where $\Delta T = 0.1\,\mathrm{s}$ is chosen to match the sampling rate of driving data. In [14] the parameters were fitted using the continuous version of the controller. The discrete version provides a time base for representing discrete control actions.

To fit the parameters, all the driving events were sliced in blocks $2\,\mathrm{s}$ long. For each of the blocks, the parameters K_f, K_n and K_i were fitted using the Moore-Penrose pseudo-inverse matrix, obtaining a distribution of fitted parameters. In the present analysis, the near and far point distances are chosen to be $d_n = 6\,\mathrm{m}$, $d_f = 30\,\mathrm{m}$ respectively. These values were found to overall produce a higher clustering density in the parameter distribution (Fig. 1). The slice duration of $2\,\mathrm{s}$ was chosen according to this same criterion. Considering that we are representing a human control system and that parameter identification in closed-loop is well known to be prone to dispersion (due to actions related to disturbance rejection), the clustering density of the distribution of the fitted parameters appears very high – Fig. 1 first column. The distribution of parameters suggests that it can be fitted by a three dimensional Gaussian model – Fig. 1 second column – which yields mean values ($K_f = 1.0826$, $K_n = -0.2228$, $K_i = 0.0415$). The distribution shows that sign of K_i is ill-defined. It is not clear if it is positive, negative or zero. A negative value of K_i would mean that the controller would increase lane offsets instead of decreasing them. K_n has clearly a negative sign. Thus, as the parameter fitting seems consistent, it suggests that there is a flaw not in the identification of the parameters but in the model itself. It appears that these data processing techniques are able to extract patterns from driving data, even if the model is not the most appropriate one. The most likely reasons for this are: the pulse like nonlinear nature of steering signals, and the evidence that the CNS operates on a HOCL scheme [18].

The eigenvalues of the Salvucci and Gray model, working in closed-loop with the vehicle model, according the the fitted parameters are: $(-0.078 \pm 1.082i,\ -0.357,\ 0.065 \pm 0.225i)$. Thus the system is unstable with the fitted parameters from NDD – one pair of conjugated complex eigenvalues have positive real part.

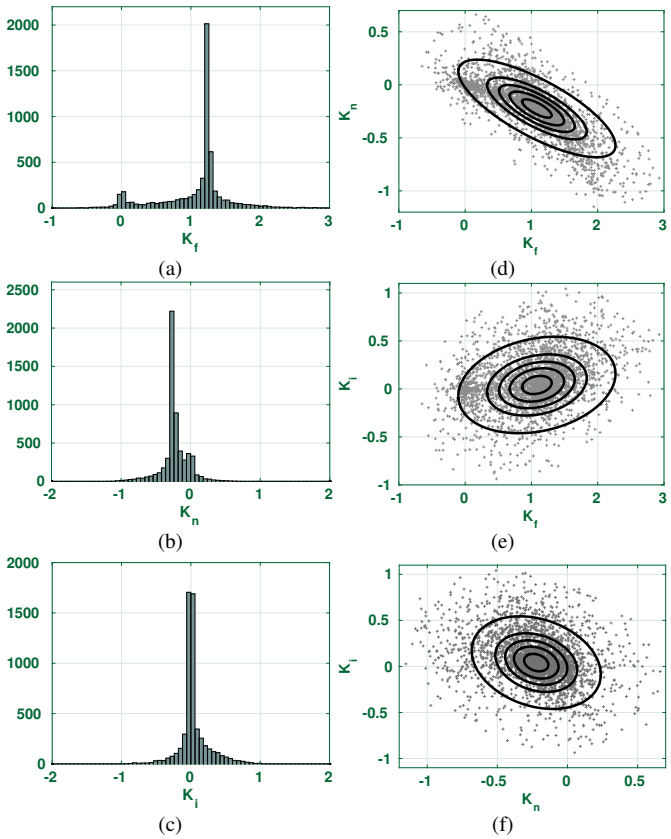

Fig. 1: Subfigures (a), (b), (c): Distribution of each of the fitted parameters K_f, K_n, K_i. Subfigures (d), (e), (f): Projections for each parameter pair with the fitted Gaussian model contour lines. The outer ellipses enclose a confidence region of 95%.

IV. Pulse extraction and analysis

A. Identification of natural pulses

Regarding the nature of the driver's motor primitives, here it is first conjectured that the steering angle signal of a driver can be described as a combination of a *ramp function*, required when taking a curve, a *bump function*, which changes the heading of the vehicle, and a *ripple function*, which brings about a lateral offset shift (Fig 3a). These signals are referred as *elementary steering pulses*, and any superposition of them as a *complex steering pulse*. It is shown that steering angle signals, recorded from driver in real road conditions, can be constructed as a sparse representation of *complex steering pulses*, and that the *complex steering pulses* found in real data are linear combinations of the same *elementary steering pulses*. This will justify the use of the proposed control scheme (9). To extract the *elementary steering pulses* from the NDD feature extraction methods are applied.

When identifying the *elementary steering pulses* in the steering angle signal, the well known technique of singular value decomposition (SVD) will be used [20]. This technique has the advantage of extracting the natural pulses from the data without any prior assumption about the pulse shapes. However, it does not provide a suitably sparse representation. The data shows that the nature of the steering signal pulses is sparse in human lane keeping control. Once the pulses are identified,

a matching pursuit dictionary [21] will be built with them. The matching pursuit algorithm will reconstruct the signal as a sparse superposition of the dictionary elements.

The adopted approach is to slice each signal into sub-samples of 1 s of duration – since it is verified that for human lane keeping pulses shorter than 1 s are typical. From the slices, a two-dimensional matrix is built by joining them in a matrix M, and principal component analysis SVD [20] is employed. The results are found to be very similar for all the driving events, and for a chosen driving event they are displayed in Fig. 2. The most dominant mode is a flat curve which contains 84% of the energy of the signal. This flat curve is responsible of dealing with the geometry of the road (compare 2a with 2c and 2d) and is the only pulse that clearly has a constant offset in amplitude (2b). The flat curve is followed by a *ramp*, a *bump* and a *ripple pulse* of smaller energy content. These three are the steering primitives or *elementary steering pulses* above hypothesized.

The given analysis also suggests a way to detrend the data, as the main interest is to describe human lane keeping and not how humans follow a particular road geometry. From the SVD output (matrices U, Σ, V such that $U\Sigma V^\top = M$), the rows and columns corresponding to the first mode (flat curve) are eliminated (reduced $\hat{U}, \hat{\Sigma}, \hat{V}$), obtaining a detrended signal with almost no road geometry content ($\hat{M}$ such that $\hat{M} = \hat{U}\hat{\Sigma}\hat{V}^\top$). Thus it is possible to preserve the frequency and amplitude of the pulses for posterior analysis (Fig. 2d). After detrending, the relative energies of the *ramp*, *bump* and *ripple* are 48%, 22% and 10% respectively. So the three main modes account for 80% of the energy of the detrended signal.

In this paper it is verified that the human-driver performs non-symmetric pulses. However, as the given analysis yields equivalent results for all the driving data, it serves to further justify the hypothesis of *elementary steering pulses* and hypothetize their shapes. The normalized pulses (*ramp* δ_1, *bump* δ_2 and *ripple* δ_3) can be described analytically according to the haversine function (Fig. 3a):

$$\begin{cases} \delta_1(t, Tp) = 1/2 \cdot (1 - \cos(\pi/T_p)t) & \text{if } 0 < t < T_p \\ 1 & \text{otherwise} \end{cases} \quad (3)$$

$$\begin{cases} \delta_2(t, Tp) = 1/2 \cdot (1 - \cos(2\pi/T_p)t) & \text{if } 0 < t < T_p \\ 0 & \text{otherwise} \end{cases} \quad (4)$$

$$\begin{cases} \delta_3(t, Tp) = 4/(3\sqrt{3}) \cdot \sin(2\pi/T_p t) \cdot \delta_2(t, Tp) & \text{if } 0 < t < T_p \\ 0 & \text{otherwise} \end{cases} \quad (5)$$

where T_p is the activation time span of the pulse or pulse duration (Fig. 3). δ_1 produces a change in the yaw-rate of the vehicle that serves to follow the geometry of the road. δ_2 produces a change on the yaw-angle. It is used to adjust the heading of the vehicle in lane keeping. And δ_3 corrects lateral offset deviations from the centre of the lane.

B. Duration of the asymmetrical steering pulses:

Regarding the question of what is the typical pulse activation span time T_p of a human driver, the possibility of these pulses to be asymmetrical is contemplated. In previous literature, only symmetrical pulses have been considered [13]. While working with detrended signals, essentially devoid of road geometry content, it is assumed that the *ramp* pulse has no relevance and it may only be used to shape *bumps* by joining a rising and a falling *ramp*. The *ripple* can be constructed in the same way by joining two *bumps*, so the

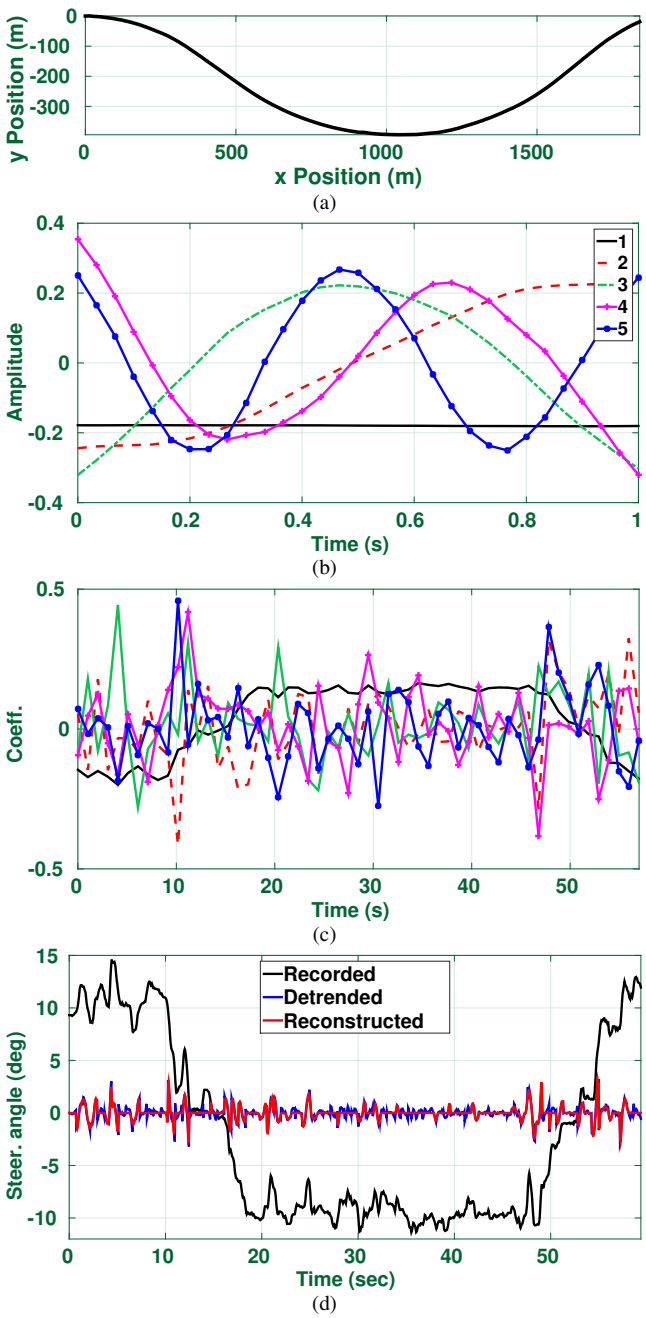

Fig. 2: (a): Road geometry for one chosen driving event (event 30 of driver A). (b): The five dominant modes of the steering signal analyzed in 1 s slices. (c): Time history of the linear combinations to describe the signals with the modes. (d): Recorded steering signal for the given driving event, along with the detrended version and the reconstruction through matching pursuit – using 60 pulses.

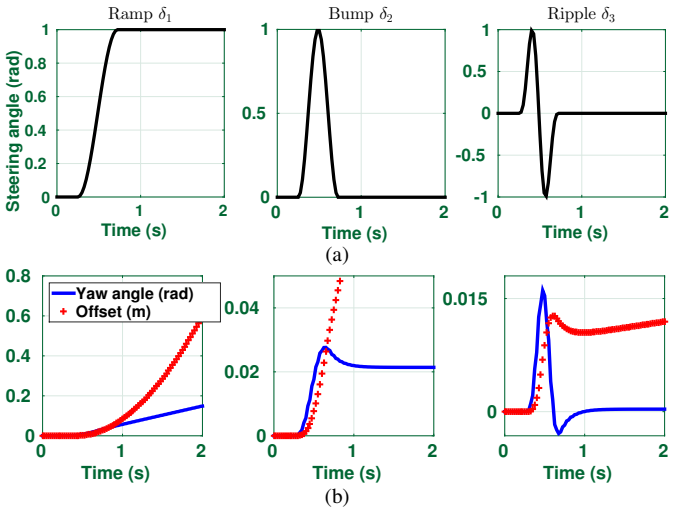

Fig. 3: Row (a): Examples of normalized *ramp function*, *bump function* and *ripple function* with $T_p = 0.5\,\mathrm{s}$ of activation each. Row (b): Responses for each of the pulses. The dashed line shows the yaw angle in radians while the sign markers show the offset from the centre of the road in meters.

most crucial pulse for lane keeping is the *bump*, as all pulse activity can be reconstructed by a superposition of *bumps*. Building a matching pursuit dictionary of asymmetrical *bumps* of different rising and falling time – rising and falling duration from $0.05\,\mathrm{s}$ to $1.5\,\mathrm{s}$ as in the detrended data there are not longer pulses and shorter pulses are regarded as noise – and running the matching pursuit algorithm over the 200 driving events, the histogram of chosen rising and falling time is obtained (Fig. 4a). This displays the selected pulse duration by the algorithm to obtain an optimal reconstruction of the signal. The rising part tends towards a shorter duration than the falling part, the latter also displaying more variability. The distribution of the mean rising and falling time of the pulses for each driving event exhibits differences among drivers. Drivers A and B use shorter pulses, especially driver B, which is the most distinct driver compared to the others (Fig. 4c). For all the drivers, the relationship between rising and falling time is inverse – the quicker the driver makes the initial *ramp*, the slower they make the reverse *ramp*. We hypothesize that the rising and falling pulse duration can be used to classify different driving states.

C. Open-loop vs. closed-loop control

According to the above, it is proposed that the driver performs an initial response to a potential conflict, by performing a first initial quick adjustment according to an open-loop scheme – the quicker rising part of the *bump* shaped pulse. After this adjustment has been made, that due to its open-loop nature will result in a over- or under-correction, the driver will perform a falling *ramp* in closed-loop. This falling *ramp* will have a different duration depending on how good the initial open-loop guess was. Thus its length has a higher variance than the rising part. In the proposed model, the rising *ramp* will correspond to a learned pattern (pre-cognitive action [14]), while the falling *ramp* to a smoother adjustment relative to the current driving scenario and the magnitude of the error produced by the first *ramp*. It is expected that the more imminent the potential conflict, the faster the driver will tend to execute the first *ramp*, and the more error will occur resulting in a longer closed-loop correction. The mechanism proposed is consistent with the presented signal analysis, and also is consistent with known mechanisms of the CNS. Specifically, the process is analogous to the way in which the human eye tracks a target. It first produces an quick saccade, to make a first approach to the target, and then smaller saccades that occur $0.15 - 0.3\,\mathrm{s}$ after [19] [22]. Also, experimental research has shown that the CNS uses a combination of open-loop and closed-loop control [18], and it has been found [23] that control only via open-loop cannot reproduce human motor behaviour. Open-loop systems are poor controllers, although they have the advantage of responding quicker. Since research suggests that the human visual and motor systems work on an open-closed- loop scheme, it is reasonable to believe that steering pulses do so too.

D. Measures of lane keeping error

Regarding the question of what makes the human driver trigger a pulse, lane keeping and driver performance metrics are examined. Different lane keeping metrics have been defined and considered for human lane keeping, for example, the time to lane crossing (TTLC) [24], the yaw-rate error (YRE) [25] and the near point angle in the two-point model [6]. Here, an alternate formulation of the YRE is defined, which is called the *critical normalized yaw-rate* (CNYR). The CNYR is easier to correlate to pulse amplitude than the YRE, although the conceptual meaning of the metric is the same. Its definition follows. First the critical yaw-rate is considered,

$$\dot{\psi}^{\mathrm{R}}_{\mathrm{crit}} = \frac{2U \sin \phi_{\mathrm{R}}}{d_{\mathrm{R}}} \tag{6}$$

where U is the velocity of the vehicle, ϕ_{R} is the azimuth angle, i.e., the angle difference between the yaw angle and the right boundary point at the distance of a far point [25]. The far point distance depends on the speed of the vehicle and a selected preview time. In the simulations, as the speed of the vehicle is mostly constant, a fixed far point distance is selected. d_{R} is the distance from the right front wheel of the vehicle to the same boundary point. From (6) it is defined the right boundary margin,

$$m_{\mathrm{R}} = \dot{\psi} - \dot{\psi}^{\mathrm{R}}_{\mathrm{crit}} \tag{7}$$

with $\dot{\psi}$ the yaw rate. When $m_R < 0$, the vehicle has engaged in a trajectory that if sustained, it would eventually take the vehicle outside the right road boundary at the distance of the far point. In an analogous way the left boundary margin m_{L} is defined. The critical yaw-rate, is the yaw-rate at which the vehicle would exit the right or left boundary at the predefined distance $d_{R,L}$ if keeping the same speed. The right or left boundary margins just show how far the current trajectory is from the critical trajectories.

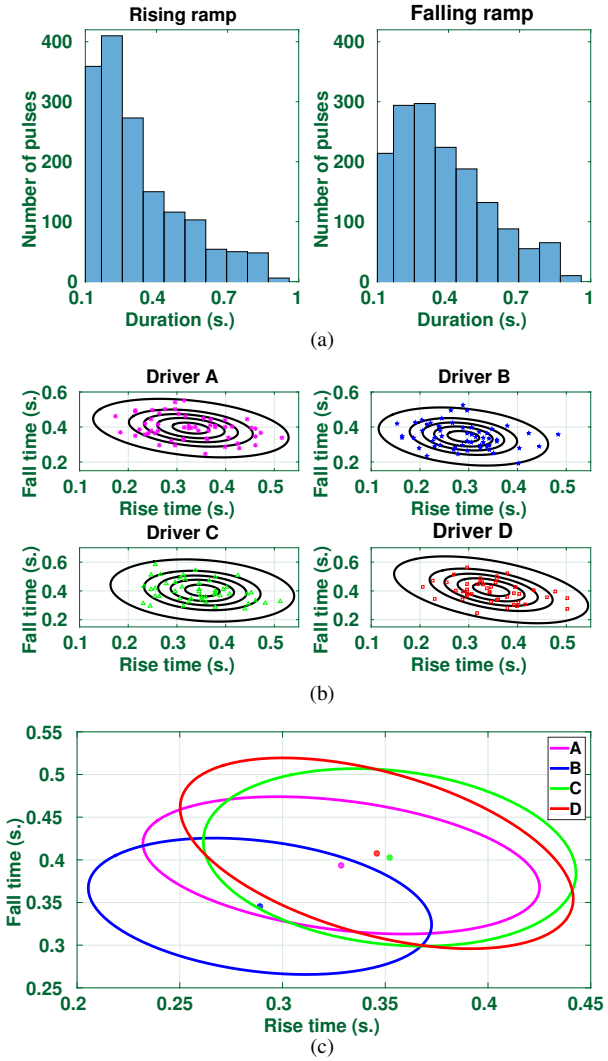

Fig. 4: (a) Histogram of rising and falling duration span of the *bumps* chosen by the matching pursuit algorithm over 200 driving events. (b) Distribution of the mean rising and falling duration time over the same driving events tabulated by driver. The mean values after fitting by a Gaussian distribution are: $A : (0.3286, 0.3935)$, $B : (0.2890, 0.3456)$, $C : (0.3521, 0.4029)$, $D : (0.3458, 0.4077)$. The outer ellipse corresponds to a confidence region of 95%. (c) Comparison of the ellipses for each driver that enclose a 50% confidence region and their centres.

From (6) the CNYR follows:

$$\chi = \frac{\dot{\psi} - 1/2\left(\dot{\psi}^R_{\text{crit}} + \dot{\psi}^L_{\text{crit}}\right)}{1/2\left(\dot{\psi}^R_{\text{crit}} - \dot{\psi}^L_{\text{crit}}\right)} \tag{8}$$

This error metric is zero whenever the yaw-rate is at equal distance from both the left and right critical yaw-rates, and its value is (≤ -1 or ≥ 1) when the vehicle is in a lane exiting trajectory at the far point, left or right respectively. In order to validate the detrending procedure used, the relationship between the CNYR and the amplitude of the pulses reconstructed by the matching pursuit algorithm over the detrended steering signal is compared (Fig 5). This is done working over the reconstructed signal through matching pursuit, which allows for a better identification of the starting and end time of the pulses and their amplitude. Fig. 5a shows the amplitude of the error produced by a steering *bump*. Here we display how a steering correction, performed in response to an unknown cause, produces an increase in the CNYR error. A steering *bump* changes the heading of the vehicle so this translates into increase in the error. This relationship, although trivial, is tested to further verify that the detrending method did keep the relevant characteristics of the data. Fig. 5b shows the reverse relationship, which is the one of interest: the CNYR error is displayed vs. the correcting pulse, done by the driver after the error is perceived in order to nullify it. Some representative cases of the relationship between CNYR and steering response to CNYR are shown in Fig. 6.

In general, for all the driving events, the steering angle of the driver goes in the direction that neutralizes the CNYR, although this does not happen for all the duration of the event. So there are a number of cases in which the CNYR does not account for the steering action undertaken. The driver may not be responding all the time to lane-keeping needs. Some of the steering pulses may be due to noise in the driver behaviour, vehicle or data collection methods, and some of the driver actions may be due to other type of precondition such as traffic contingencies, interaction with other vehicles on the road driver or even driver distraction.

In Fig 5a, 79% of the pulses generate a CNYR of the expected sign – positive pulses generate later positive error – after a lag of $0.3 - 0.7\,\text{s}$. This relationship corresponds mostly to vehicle response, but it is relevant the fact that the signal pre-processing – SVD and matching pursuit – did preserve it. The driver, in order to rectify an error, must first change the heading of the vehicle, producing a higher CNYR. A steering *bump* in the opposite direction gets the heading back within the right and left boundary margins (m_{R} and m_{L}). And in Fig. 5b, the number of pulses occurring in the expected quadrant location – positive error induces a *bump* of negative amplitude is 74% – a little lower than the previous relationship. This correcting pulse is detected after a lag of $0.1 - 0.5\,\text{s}$ from the error preceding peak.

The same direct relationship has been tested for the two error measures, regarding human lane keeping, of the two point model: θ_n and $\dot{\theta}_n$. In the case of θ_n the relationship is very weak. Choosing only the driving events in which the steering action to near point angle error occurs in the direction that neutralizes it at least 60% of the times, a much more inhabited plot results (Fig 7a). In the plot the percentage of dots in the expected quadrant – a positive value of θ_n is corrected by a positive amplitude steering pulse – is only of 62%. This percentage appears to be very low considering how the cases where selected, and suggests that there is no correlation at all. For $\dot{\theta}_n$ the correlation looks present but very weakly – 65% of corrections in the neutralizing direction and plot slightly more populated (Fig. 7b).

Nevertheless, even if the driver would not be directly responding to these error measures, the relationship must be there in an indirect way. The driver needs to keep the

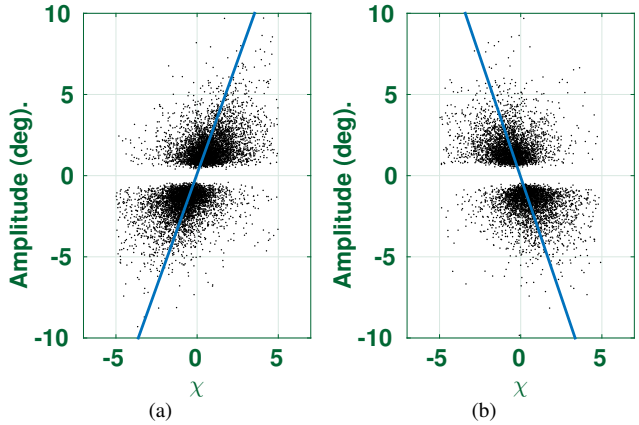

Fig. 5: (a): Amplitude of the steering pulses chosen by matching pursuit against the CNYR error generated by them. (b): Amplitude of the pulses against the error they respond to. The fitted lines display the trend of the relationship. In both cases, pulses of small amplitudes are discarded by the matching pursuit algorithm, which selects only 60 pulses from the dictionary.

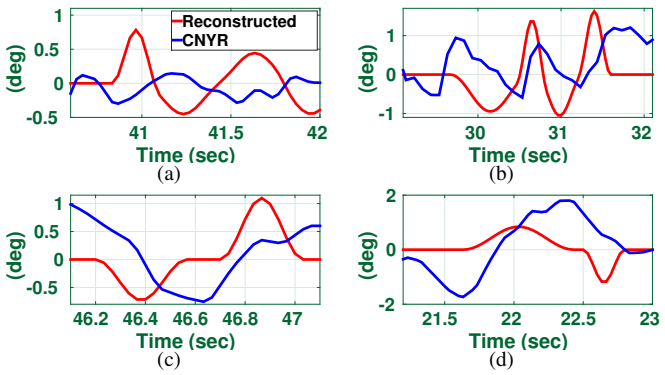

Fig. 6: (a-d): Examples of CNYR neutralizing actions after a time lag of variable duration for drivers $(A-D)$ respectively. The start of the EPSs is detected by the matching pursuit reconstruction of the detrended steering signal.

vehicle between the lane boundaries, whatever strategy he or she may utilize. The relationship has not been detected by signal processing probably because θ_n and $\dot{\theta}_n$ signals are much more dependent on road geometry, cross-wind steering counter-reactions or much more affected by noise in the data. Furthermore, it has been mentioned that the driver may not be persistently responding to errors in a continuous way, as this will involve a high *observational workload* [10] and *steering action workload*. On the other hand, CNYR does not require constant monitoring as it is based on a preview distance or time. In any case, the *elementary steering pulse-*χ relationship seems to be most consistent.

V. HOCL CONTROL SCHEME

A. 'Act-and-wait' Control

The 'act-and-wait' method is a relatively new concept in control theory, although very familiar in everyday human experience; when controlling a system subject to both uncertainty

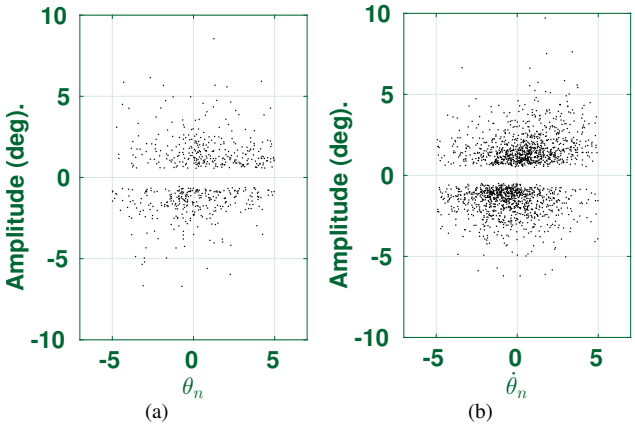

Fig. 7: (a): Amplitudes of matching pursuit detected *elementary steering pulses* vs. near angle errors (θ_n). (b): Amplitudes of matching pursuit detected *elementary steering pulses* vs. derivative of near angle errors ($\dot{\theta}_n$).

and time-delay, there are advantages in waiting to assess the effect of a control action before acting again. According to [7], for a linear plant with delay, the method simplifies the process of stabilization by pole-placement and results in a finite-dimensional discrete-time linear feedback system which may be stabilized using simple pole-placement. It is shown that the waiting time should exceed the delay time. In [8] the method is successfully applied to the control of a nonlinear mechanical system, and indicates that a proportional gain can be increased significantly without losing stability, compared to a continuous controller. For steering control, it seems plausible that the same act-and-wait action can be successful, allowing the human driver to apply higher feedback gains to overcome nonlinearities (e.g. friction in the steering system) and yet preserve stability.

This hypothesis that human drivers adopt the *act-and-wait* method is not formally analysed in the current paper, but the similarity is assessed in general terms and the HOCL control scheme incorporates this concept. In particular, one expects the delay between actions (steering pulses) to exceed the drivers neuro-muscular time delay of around $200\,\mathrm{ms}$. The following designed control scheme explicitly incorporates the 'act-and-wait'concept.

B. Hybrid Control Law

In the line with the considerations of the previous section, the HOCL pulse control scheme is now defined:

$$\begin{cases} \delta(t) = \bar{K} \cdot \bar{C}\left(\bar{E}(t)\right) & \text{if } R\left(\bar{E}(t)\right) \leq T_h \\ \delta(t) = K_{rb} \cdot \delta_{rb}(t - t_0, T_{rb}) \cdot F\left(\bar{E}(t)\right) & \text{otherwise} \end{cases} \tag{9}$$

where $\bar{K}$ is a vector of parameters, $\bar{C}$ a vector function controller (working in closed-loop, linear and continuous/discrete) that acts according to another vector function of selected errors $\bar{E}$, when these are below the threshold T_h relative to a function R. When R is above the threshold at a given time t_0, a rising *bump* δ_{rb} is performed (open-loop) of rising duration T_{rb}. For the duration of the rising *bump* $\bar{C}$ is interrupted, then the

control is passed back to $\bar{C}$ until the termination of the pulse. The amplitude of δ_{rb} depends on a constant parameter K_{rb} and on the magnitude of the errors according to a function F. The HOCL control scheme also assumes a wait time T_w during which may not trigger further pulses. This is further justified by the sparsity of higher amplitude pulses, as shown in the matching pursuit reconstruction (Fig 2d). The same HOCL scheme can also be applied with different types of *elementary steering pulse* acting on superposition. Here we consider a HOCL that triggers *elementary steering pulses* according to the right or left boundary margins (7) and the closed-loop control is the Salvucci and Gray model,

$$\begin{cases} \dot{\delta}(t) = K_f\dot{\theta}_f + K_n\dot{\theta}_n + K_i\theta_n & \text{if } \min(m_L, m_R) < 0 \\ \delta(t) = K_{rb}\delta_{rb}(t - t_0, T_{rb}) \cdot (m_R - m_L) & \text{otherwise.} \end{cases} \tag{10}$$

K_f, K_i are taken as in the above fitted parameters (Fig 1), and $T_{rb} = 0.3$ according to the rising time results (Fig. 4). The parameters K_n – which as fitted through NDD was leading to instability – and K_p are fitted using a genetic algorithm. The objective function evaluates performance based on lane keeping quality and smoothness steering: $\mathcal{P} = \frac{1}{N}\sum_{t=t_1}^{t=t_N}\left(y_k + C\dot{\delta}_k\right)$, where N is the number of time samples $t_1 \dots t_N$, y_k is the lateral offset from the centre of the lane and $\dot{\delta}_k$ the steering rate in $\mathrm{rad/s}$ at each time sample. C is a constant set empirically to 100 which relates both terms in the objective function. With the given setup the optimized parameters are $K_n = 0.1105$ and $K_p = 0.0119$.

The wait time T_w has been set to $0.5\,\mathrm{s}$. Although this value has not been optimized, it has been observed that much longer or shorter wait times were less effective. With longer wait times the pulse control offers reduced error correction, whereas with shorter wait times the closed-loop part of the model does not have time to counterbalance the effect of the pulses. In this case the trajectory becomes too jerky, which forces the triggering of continuous pulses to rectify this, as the threshold is continuously surpassed. So this example can be considered a first implementation of the *act-and-wait* concept in the context of steering control [7] [8].

In simulation, the above implementation of HOCL model performs significantly better than the Salvucci and Gray model with the fitted parameters from NDD. Running the Salvucci and Gray model and (10) in the road geometry of the same driving event as in Fig. 2, it is shown that Salvucci and Gray model becomes unstable after about half of the event has been covered (Fig. 8a). The hybrid model, although presenting a jerky spot at the same point where Salvucci and Gray model becomes unstable, is able to recover the stability and proceed to the end of the event within the lane boundaries (Fig. 8b). Testing also the HOCL in a straight track with an initial lane offset of $3\,\mathrm{m}$ to the left, the simulations show that the vehicle is able to neutralize the offset and stabilize at the centre of the lane (Fig. 8b). The Salvucci and Gray model was also tested in a straight track, and even without initial offset the noise in the simulation was enough to destabilize it, and thus not presented in the figure.

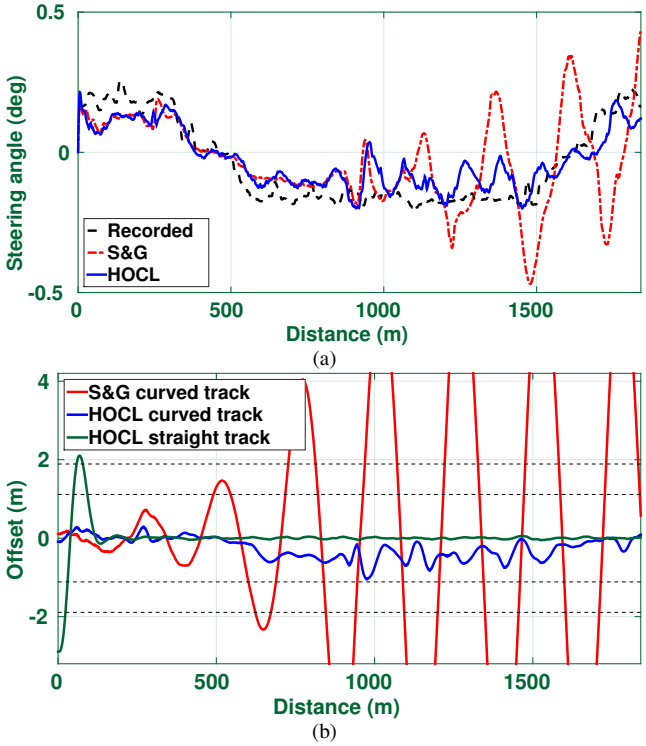

Fig. 8: (a) Recorded steering signal for driving event 30 of driver A, along with the steering signals of Salvucci and Gray model and the HOCL example (10) (b) Lane offset from the centre of the road for the HOCL example in the curved geometry of the same driving event, and on a straight track with an initial offset of $3\,\mathrm{m}$. Negative offsets are to the left and positive offsets to the right. The outer margins are the lane boundaries, while the inner margins mark when the wheels of the vehicle reach to the lane boundaries.

VI. Conclusion

This paper has focused on describing patterns of driver behaviour that can lead to representative biofidelic modelling of human driving. Firstly, the hypothesis is developed, that the steering signal is governed by basic motor primitives. Through the use of machine learning techniques and detailed signal processing, it has been possible to extract patterns from steering signals that support this claim. Furthermore, the basic motor primitives for human lane keeping, which are referred to as *elementary steering pulses*, have the shape of an *asymmetrical bump function*. These findings suggest that the steering action is well described by an HOCL scheme, which is further supported by previous research on the CNS. The HOCL control scheme, designed through a *data-driven modelling* approach using NDD and based on pulses, may also account for visual attention switching and opens new ways to implement level 2 or level 3 automation assistance controls.

Furthermore, fitting the parameters with NDD of a well known steering control model, the Salvucci and Gray model, led to a consistent set of parameters from the optimization point of view. Nevertheless, the Salvucci and Gray model is unstable with the fitted parameters, which suggests that this very simple model does not characterize the way in which

humans perform steering control. Pure linear type closed-loop control systems cannot easily accommodate for visual attention switching as the HOCL does. The presented example, shows that adding pulse control to a linear closed-loop control law can stabilize unstable parameters. Regarding the fact of which are the error-metrics that relate more faithfully to the way in which humans trigger *elementary steering pulses*, it was found that the YRE metric, in particular the alternate formulation of CNYR, is a possible representative. Some examples have been given of how performance metrics are used already in the industry to monitor driver vigilance.

Further work should be aimed towards the study of the most suitable control systems based on the general HOLC model as well the design of control laws, that modify the human performed steering pulses, improving thus the performance and the safety of the driving, including the possibility of manipulating driver attention levels. In general, vehicle automation research aims at increasing the level of automation. But this work aims at increasing the level of security and performance of the driver by assisting with *partial* or *conditional automation*. One option would be via the addition of pulses to those performed by the driver. The aim of these pulses would be to modulate the effective amplitudes and test whether the driver responds accordingly. This is the subject of ongoing research. This research has the potential for high impact in the intelligent transportation industry, road safety and development of vehicle automation.

Acronyms	
CNS	*Central nervous system*
HOCL	*Hybrid open-closed- loop*
NDD	Naturalistic driving data
SAE	Society of Automotive Engineers
SVD	*Singular value decomposition*
TTLC	*Time to lane crossing*
YRE	*Yaw-rate error*

TABLE I

Notation	
δ	*Steering angle*
$\delta_1, \delta_2, \delta_3$	*Ramp function*, *bump function* and *ripple function* respectively.
δ_{rb}	*Rising bump function*
$\theta_{n,f}$	*Angle to near (n) or far (f) point (from center of vehicle)*
$\phi_{R,L}$	*Azimuth angle to right (R) or left (L) boundary point*
χ	Critical normalized yaw-rate (CNYR)
ψ	*Yaw-angle*
$\dot{\psi}_{R,L}$	*Critical yaw-rate to right (R) or left (L) boundary point*
$d_{n,f}$	*Distance to near (n) or far (f) point (from center of vehicle)*
$d_{R,L}$	*Distance from right (R) or left (L) wheel to right or left boundary point*
$m_{R,L}$	Right (R) or left (L) boundary margin
$\mathcal{P}$	Driving performance metric
U	*Velocity of the vehicle*

TABLE II

REFERENCES

[1] C. C. Macadam, "Understanding and modeling the human driver," *Vehicle System Dynamics*, vol. 40, no. 1-3, pp. 101–134, 2003.

[2] M. Plöchl and J. Edelmann, "Driver models in automobile dynamics application," *Vehicle System Dynamics*, vol. 45, no. 7-8, pp. 699–741, 2007.

[3] M. Kondo and A. Ajimine, "Drivers sight point and dynamics of the driver-vehicle-system related to it," SAE Technical Paper, Tech. Rep., 1968.

[4] E. Donges, "A two-level model of driver steering behavior," *Human Factors: The Journal of the Human Factors and Ergonomics Society*, vol. 20, no. 6, pp. 691–707, 1978.

[5] M. Land and J. Horwood, "Which parts of the road guide steering?" *Nature*, vol. 377, no. 6547, pp. 339–340, 1995.

[6] D. D. Salvucci and R. Gray, "A two-point visual control model of steering," *Perception-London*, vol. 33, no. 10, pp. 1233–1248, 2004.

[7] T. Insperger, "Act-and-wait concept for continuous-time control systems with feedback delay," *Control Systems Technology, IEEE Transactions on*, vol. 14, no. 5, pp. 974–977, 2006.

[8] T. Insperger, L. L. Kovács, P. Galambos, and G. Stépán, "Increasing the accuracy of digital force control process using the act-and-wait concept," *Mechatronics, IEEE/ASME Transactions on*, vol. 15, no. 2, pp. 291–298, 2010.

[9] T. Victor, J. Bärgman, M. Hjälmdahl, K. Kircher, E. Svanberg, S. Hurtig, H. Gellerman, and F. Moeschlin, "Sweden-michigan naturalistic field operational test (semifot) phase 1: Final report," *SAFER Report*, vol. 2, 2010.

[10] T. Gordon and Y. Zhang, "Steering pulse model for vehicle lane keeping," in *Computational Intelligence and Virtual Environments for Measurement Systems and Applications (CIVEMSA), 2015 IEEE International Conference on*. IEEE, 2015, pp. 1–5.

[11] P. Morasso, "Spatial control of arm movements," *Experimental brain research*, vol. 42, no. 2, pp. 223–227, 1981.

[12] W. Abend, E. Bizzi, and P. Morasso, "Human arm trajectory formation." *Brain: a journal of neurology*, vol. 105, no. Pt 2, pp. 331–348, 1982.

[13] O. Benderius and G. Markkula, "Evidence for a fundamental property of steering," in *Proceedings of the Human Factors and Ergonomics Society Annual Meeting*, vol. 58, no. 1. SAGE Publications, 2014, pp. 884–888.

[14] T. Gordon and K. Srinivasan, "Modeling human lane keeping control in highway driving with validation by naturalistic data," in *Systems, Man and Cybernetics (SMC), 2014 IEEE International Conference on*. IEEE, 2014, pp. 2507–2512.

[15] O. Nakayama, T. Futami, T. Nakamura, and E. R. Boer, "Development of a steering entropy method for evaluating driver workload," SAE Technical Paper, Tech. Rep., 1999.

[16] M. Lidberg and T. Gordon, "Automated driving and autonomous functions on road vehicles," *Vehicle System Dynamics*, vol. 53, no. 7, 2015.

[17] D. LeBlanc, "Road departure crash warning system field operational test: methodology and results. volume 1: technical report," 2006.

[18] S. Hanneton, A. Berthoz, J. Droulez, and J.-J. E. Slotine, "Does the brain use sliding variables for the control of movements?" *Biological cybernetics*, vol. 77, no. 6, pp. 381–393, 1997.

[19] R. J. Jagacinski and J. M. Flach, *Control theory for humans: Quantitative approaches to modeling performance*. CRC Press, 2003.

[20] V. C. Klema and A. J. Laub, "The singular value decomposition: Its computation and some applications," *Automatic Control, IEEE Transactions on*, vol. 25, no. 2, pp. 164–176, 1980.

[21] S. G. Mallat and Z. Zhang, "Matching pursuits with time-frequency dictionaries," *Signal Processing, IEEE Transactions on*, vol. 41, no. 12, pp. 3397–3415, 1993.

[22] L. Young and L. Stark, "Variable feedback experiments testing a sampled data model for eye tracking movements," *Human Factors in Electronics, IEEE Transactions on*, no. 1, pp. 38–51, 1963.

[23] N. Bhushan and R. Shadmehr, "Computational nature of human adaptive control during learning of reaching movements in force fields," *Biological cybernetics*, vol. 81, no. 1, pp. 39–60, 1999.

[24] C.-F. Lin and A. G. Ulsoy, "Time to lane crossing calculation and characterization of its associated uncertainty," *Journal of Intelligent Transportation Systems*, vol. 3, no. 2, pp. 85–98, 1996.

[25] T. Gordon, A. Blankespoor, M. Barnes, D. Blower, P. Green, and L. Kostyniuk, "Yaw rate error–a dynamic measure of lane keeping control performance for the retrospective analysis of naturalistic driving data," in *21st International Technical Conference on the Enhanced Safety of Vehicles, Stuttgart, Germany*, 2009, pp. 09–0326.